Economic Geology
Vol. 96, 2001, pp. 957–971

The Alteration Box Plot: A Simple Approach to Understanding the Relationship between Alteration Mineralogy and Lithogeochemistry Associated with Volcanic-Hosted Massive Sulfide Deposits

Ross R. Large,† J. Bruce Gemmell, Holger Paulick,*

Centre for Ore Deposit Research, School of Earth Sciences, University of Tasmania, GPO Box 252-79, Hobart, Tasmania 7001, Australia

and David L. Huston

Australian Geological Survey Organisation, GPO Box 378, Canberra, ACT 2601

Abstract

Zonal alteration is a common feature in volcanic rocks surrounding sea-floor massive sulfide deposits. Alteration indexes, such as the Ishikawa alteration index (AI) and the chlorite-carbonate-pyrite index (CCPI), have been developed to measure the intensity of sericite, chlorite, carbonate, and pyrite replacement of sodic feldspars and glass associated with hydrothermal alteration proximal to the orebodies. In this paper a simple graphical representation of the Ishikawa AI plotted against the CCPI, termed the "alteration box plot," is used to characterize the different alteration trends related to massive sulfide ores and to assist in the distinction of volcanic-hosted massive sulfide (VHMS)-related hydrothermal alteration from regional diagenetic alteration. Although there are some limitations with the technique, a series of case studies are used to demonstrate that the alteration box plot is a powerful means of understanding the relationship between mineralogy, lithogeochemistry, and intensity of alteration in zoned alteration systems related to VHMS deposits and should assist the exploration geologist in determining vectors to the center of the ore system.

Introduction

The principal use of lithogeochemistry in exploration for volcanic-hosted massive sulfide (VHMS) deposits is to characterize the nature and degree of alteration of the volcanic rocks and to answer two questions: (1) is the alteration caused by a hydrothermal system related to a VHMS deposit? and (2) if yes, then where is the orebody in relationship to the defined altered rocks?

The first question is critically important in order to prevent the expenditure of exploration dollars on alteration zones that are unrelated to the target massive sulfide deposits. The second question is equally important because an understanding of the relationship between alteration mineralogy, lithogeochemistry, and alteration zoning can lead the explorer directly to the massive sulfide target within a complex alteration system.

The purpose of this paper is to propose a simple graphical representation of lithogeochemical data for altered volcanic rocks, which enables a better understanding of the relationship between alteration mineralogy and lithogeochemistry within the context of zoned hydrothermal alteration systems related to VHMS deposits. The usefulness of the alteration box plot will be tested on some lithogeochemical data sets from a series of zinc- and copper-rich VHMS and related deposits described elsewhere in this special issue (Rosebery, Thalanga, Hellyer, and Western Tharsis).

Alteration Indexes

The alteration box plot is a graphical representation that uses two alteration indices: the Ishikawa alteration index (AI) and the chlorite-carbonate-pyrite index (CCPI).

† Corresponding author: e-mail, Ross.Large@utas.edu.au

*Present address: Institut für Mineralogie, Lehrstuhl für Lagerstättenlehre und Leibniz Labor für angewandte Meeresforschung, TU Bergakademie, Freiberg, Brennhausgasse 14, 09596, Freiberg, Germany.

Ishikawa AI

$$AI = \frac{100\,(K_2O + MgO)}{(K_2O + MgO + Na_2O + CaO)}. \quad (1)$$

This index was defined by Ishikawa et al. (1976) to quantify the intensity of sericite and chlorite alteration that occurs in the footwall volcanics proximal to Kuroko deposits. The key reactions measured by the index involve the breakdown of sodic plagioclase and volcanic glass and their replacement by sericite and chlorite. Reactions that describe these alteration processes include:

$$\underset{\text{albite}}{3NaAlSi_3O_8} + K^+ + 2H^+ = \underset{\text{sericite}}{KAl_3Si_3O_{10}(OH)_2} + \underset{\text{quartz}}{6SiO_2} + 3Na^+, \quad (2)$$

and

$$\underset{\text{sericite}}{2KAl_3Si_3O_{10}(OH)_2} + 3H_4SiO_4 + 9Fe^{2+} + 6Mg^{2+} + 18H_2O = \underset{\text{chlorite}}{3Mg_2Fe_3Al_2Si_3O_{10}(OH)_8} + 2K^+ + 28H^+. \quad (3)$$

The first reaction is typical of sericite replacement of albite in volcanic rocks in the outer parts of the alteration system (e.g., Date et al., 1983; Eastoe et al., 1987). The second reaction is important close to massive sulfide mineralization in footwall pipe zones where chlorite-rich assemblages become dominant over sericite-rich assemblages (e.g., Sangster, 1972; Lydon, 1988; Large, 1992; Lentz, 1999; Schardt et al., 2001). Reaction (2) involves a loss of Na_2O (and CaO) and a gain of K_2O, whereas reaction (3) involves a loss of K_2O and gains in FeO and MgO, on the basis of constant Al_2O_3.

0361-0128/01/3168/957-15 $6.00

The Ishikawa AI was devised to ratio the principal rock-forming elements gained during chlorite and sericite alteration ($MgO + K_2O$) over the elements lost and gained ($Na_2O + CaO + MgO + K_2O$). The index varies from values of 20 to about 60 for unaltered rocks and between 50 and 100 for hydrothermally altered rocks, with an AI = 100 representing complete replacement of feldspars and glass by sericite and/or chlorite.

The index has proved to be particularly useful in mineral exploration by providing a quantitative estimate of the intensity of footwall alteration related to massive sulfide deposits, increasing to maximum values in the hydrothermal vent zone below the massive sulfide ore lenses (e.g., Saeki and Date, 1980). An example from the Hellyer deposit is shown in Figure 1 (Gemmell and Large, 1992), where the AI increases from 35 to 95 from the margin to the center of the alteration pipe directly below the ore deposit. Because loss of sodium is the major chemical exchange involved in the breakdown of sodic plagioclase, there is a strong relationship between the Ishikawa AI and sodium depletion (Fig. 1). In fact many alteration studies have used sodium depletion rather than the AI as the principal measure of alteration intensity (e.g., Franklin et. al., 1975; Date et al., 1979, 1983; Hashiguchi et al., 1983; Ashley et al., 1988).

The relationship between Na_2O and the AI for a series of calc-alkaline volcanics from the Mount Read Volcanics (Blake et al., unpub. data) is shown in Figure 2a, where the broad pattern of sodium depletion that accompanies the AI increase is outlined. The data display a trend from the albite-plagioclase side of the diagram to the chlorite-sericite corner, with an increasing AI and decreasing Na_2O. In Figure 2b it is apparent that an increasing AI is also accompanied by increasing K_2O (as is expected from eq 1), with the level of K_2O enrichment dependent on the ratio of sericite to chlorite in the altered product.

There are two limitations on the use of the Ishikawa AI: the index does not take account of carbonate alteration, which can be significant in some VHMS alteration systems and may lead to a decrease in the AI, even where alteration intensity is high; and used by itself, the index does not enable separation of chlorite- from sericite-rich alteration, the two common and major zones of alteration associated with massive sulfide ores. These limitations have been overcome by introducing a second index to complement the AI.

Chlorite-carbonate-pyrite index (CCPI)

$$\text{CCPI} = \frac{100\,(\text{MgO} + \text{FeO})}{(\text{MgO} + \text{FeO} + \text{Na}_2\text{O} + \text{K}_2\text{O})}, \qquad (4)$$

where FeO is total ($FeO + Fe_2O_3$) content of the rock.

Mg-Fe chlorite alteration is typically developed close to VHMS deposits where hydrothermal temperatures and water/rock ratios are at their maxima (e.g., Franklin et al. 1981; Lydon 1988; Schardt et al, 2001). It is therefore important from an exploration perspective to develop geochemical criteria that clearly distinguish samples with elevated chlorite content within any altered volcanics data set. The above index has been designed to measure the increase in MgO and FeO associated with the Mg-Fe chlorite development, which commonly replaces albite, K feldspar, or sericite in the volcanic rock, leading to a loss of Na_2O and K_2O such as depicted in equation (3).

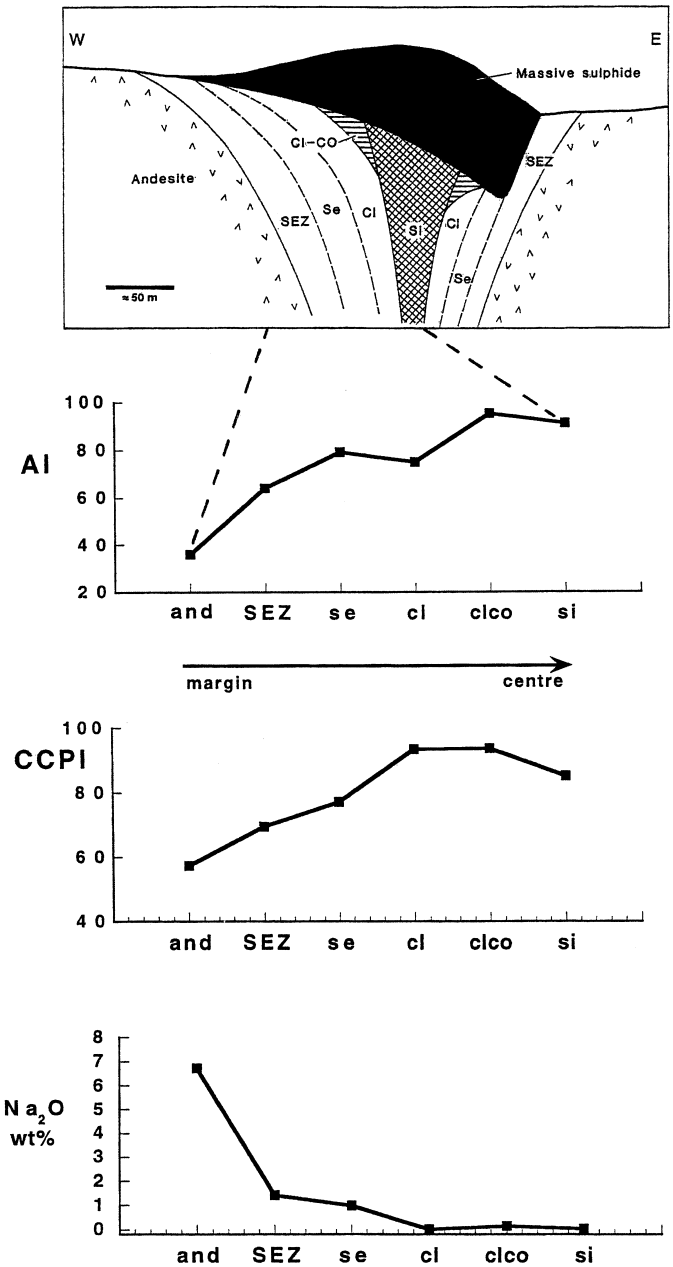

FIG. 1. Idealized cross section of the Hellyer VHMS deposit, showing the zoned footwall alteration system. Mean values of Ishikawa alteration index (AI), chlorite-pyrite-carbonate index (CCPI), and Na_2O are shown for the various alteration zones from the margin to the center of the pipe. Abbreviations: and = least altered andesite, cl = chlorite ± pyrite ± quartz, clco = chlorite > dolomite, se = strong sericite-chlorite ± pyrite, SEZ = weak sericite ± chlorite, si = quartz–chlorite ± sericite (modified from Gemmell and Large, 1992).

In addition to measuring chlorite alteration, this index is also affected positively by Mg-Fe carbonate alteration (dolomite, ankerite, or siderite) as well as pyrite, magnetite, or hematite enrichments. Because all three of the hydrothermal minerals—Fe-Mg chlorite, Fe-Mg carbonate, and pyrite—are typically developed in the inner alteration zones

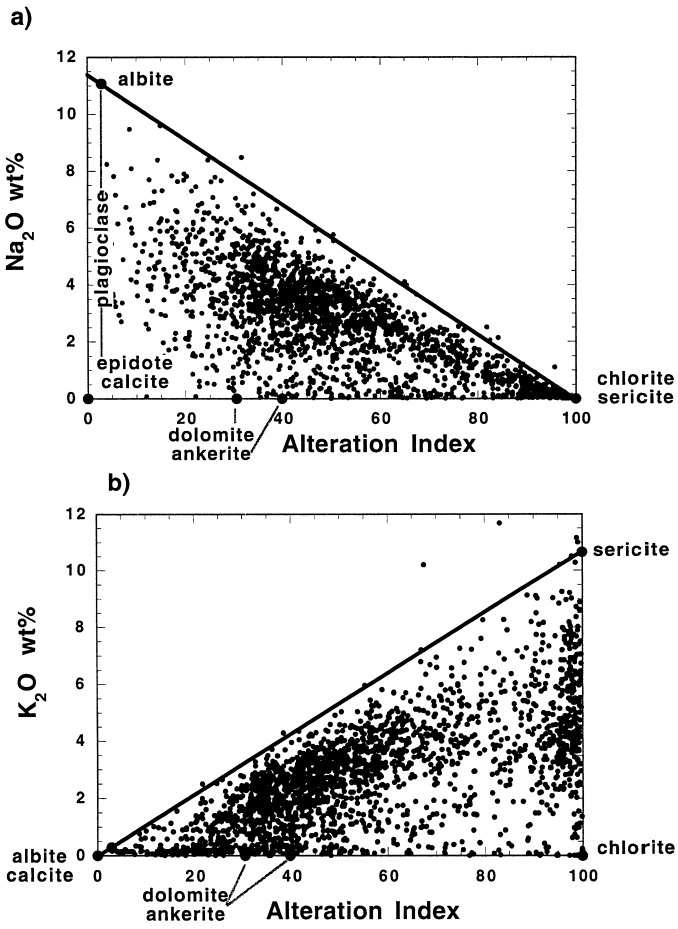

FIG. 2. Trends of AI with (a) Na_2O and (b) K_2O for a set of samples from the Mount Read Volcanics (Blake et al., unpub. data). Samples with an AI >60 are considered to be affected by alteration due to hydrothermal fluids.

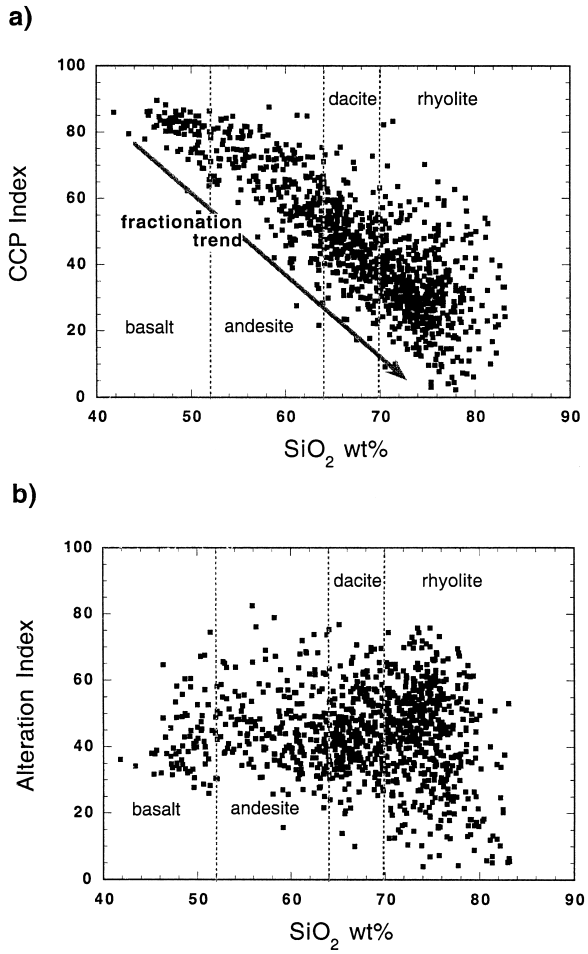

FIG. 3. Variation in (a) CCPI and (b) Ishikawa AI with SiO_2 content for a set of least altered volcanics (2 < Na_2O < 5 wt %) from the Mount Read Volcanics.

to many VHMS deposits, the CCPI is regarded as a proximal alteration index.

Lentz (1996, 1999) developed a similar index to study alteration associated with the Brunswick 6 and 12 massive sulfide deposits in the Bathurst mining camp, Canada. The composite ratio used by Lentz $(Fe_2O_{3(total)} + MgO)/(K_2O + Na_2O)$ has been modified in this study (eq 4) to make it comparable to the Ishikawa AI and vary between 0 and 100.

One important limitation of this chlorite-carbonate-pyrite index is that it is strongly affected by magmatic fractionation and primary compositional variations in the volcanic rocks. This is clearly seen in Figure 3a where the CCPI is plotted against SiO_2 for a subset of least altered volcanics from the Mount Read Volcanics (Blake et al., unpub. data). In Figure 3a it is evident that the CCPI for least altered volcanics (2 < Na_2O < 5 wt %) increases from values of around 15 to 45 in rhyolites, 30 to 60 in dacites, 50 to 85 in andesites, and 70 to 90 in basalts. This contrasts with the AI, which shows significant scatter and no obvious single trend across the same compositional range from rhyolite to basalt (Fig. 3b).

Alteration Box Plot

The alteration box plot is a combination of the Ishikawa AI plotted in the horizontal axis and the CCPI plotted in the vertical axis (Fig. 4). Least altered volcanics plot toward the center of the diagram, and hydrothermally altered volcanics plot at varying positions dependent on the principal hydrothermal minerals present. The mineral end members (albite, K feldspar, sericite, chlorite, pyrite, dolomite, ankerite, and epidote) plot along the boundaries of the box in the positions marked (Fig. 4).

Application of the alteration box plot

A series of rhyolitic volcanic samples selected from a traverse through the hydrothermal alteration system to the Hercules VHMS deposit in the Mount Read Volcanics of western Tasmania (Fig. 5) have been plotted in Figure 4. Fifteen of the samples are from the hanging-wall rhyolitic lava and volcaniclastic succession, five from the host-rock volcaniclastics, and ten from the altered footwall rhyolitic pumice breccia mass flows (Fig. 5).

Based on petrographic studies and sodium content, the least altered hanging-wall rhyolitic volcanic samples plot within the box bounded by an AI = 20 to 65 and a CCPI = 15 to 45. The progressive change with alteration along the traverse can be appreciated by comparing the plotted position of the samples in Figure 4 to the mineralogical and textural

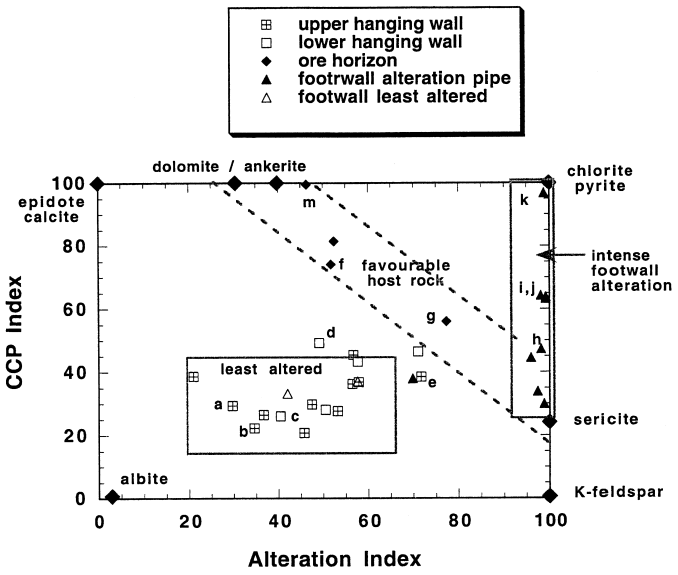

FIG. 4. Alteration box plot showing samples collected along a traverse through the alteration system to the Hercules deposit (Fig. 5). Petrographic relationship of samples marked a to m are shown in Figure 6.

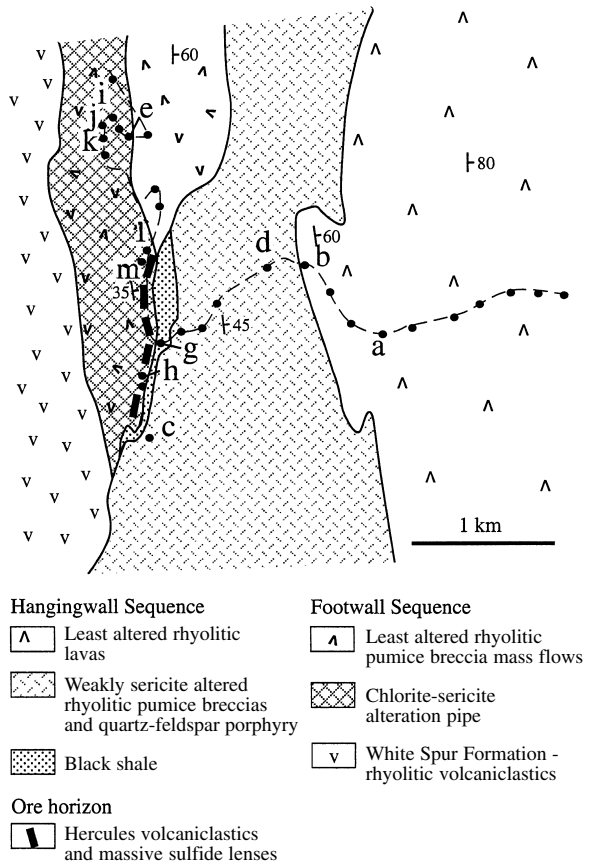

FIG. 5. Location of sample traverse and footwall hydrothermal alteration pipe associated with the Hercules deposit, western Tasmania. Geology simplified from Corbett (1986). Sample locations marked a to m are those depicted in Figures 4 and 6.

depiction in Figure 6. Hanging-wall volcanics within the least altered box have fresh albite preserved, with minor sericite and chlorite development, which is considered to relate to greenschist facies metamorphism rather than hydrothermal alteration (Fig. 6a, b, c).

Volcanics with increased sericite-carbonate alteration (Fig. 6d, f) plot above the unaltered box with increased CCPI values, whereas samples with increased sericite ± chlorite alteration plot to the right of the box due to increased AI values (Fig. 6e, g). Samples with intense sericite-chlorite from the footwall alteration zone (Fig. 5) plot on the right hand side of the diagram, where complete albite breakdown leads to an AI >90 (Fig. 6h). With increased chlorite alteration toward the center of the footwall alteration pipe at Hercules, samples plot progressively along the sericite-chlorite join with increasing CCPI values (Figs. 4 and 6i, j, k). Note that although these rocks have suffered intense alteration the outlines of replaced albite phenocrysts are still evident (Fig. 6f, h, i, j). Intense dolomite-chlorite alteration, which occurs in the footwall and ore horizon, immediately adjacent to the ore lenses, is represented by samples plotting along the chlorite-dolomite join (Figs. 4 and 6m), which have a CCPI >95 but an AI from 30 to 80. Carbonate-sericite alteration is typical of samples in the favorable stratigraphy hosting and along strike from the Hercules ore lenses, which on the alteration box plot lie along the corridor between sericite and dolomite (Figs. 4 and 6f).

In summary, this example from Hercules shows how the alteration box plot can assist in the definition of least altered volcanics and help to relate volcanic lithogeochemistry to hydrothermal mineralogy and ultimately track hydrothermal alteration from the distal to the proximal parts of the VHMS-related hydrothermal system.

Due to the fact that the CCPI varies with magma fractionation the field of least altered volcanics varies according to their composition (Fig. 7). This has major implications for understanding trends in alteration systems developed in intermediate and mafic host rocks and means that the alteration box plot must be used carefully in successions that exhibit variable volcanic compositions. This is highlighted in the case studies discussed in a later section.

Diagenetic and hydrothermal alteration trends

Diagenetic alteration of sea-floor volcanics leads to mineralogical changes that need to be discriminated from ore-related hydrothermal alteration events. The principal changes due to diagenesis is the formation of alkali-rich silicate minerals such as clays, zeolites, and feldspars (e.g., Iijima, 1974; Shirozo, 1974; Munha and Kerrich, 1980; Allen and Cas, 1990; Gifkins and Allen, 2001). In greenschist metamorphosed volcanic rocks these changes are limited to processes such as albitization, K feldspar, calcite, and epidote alterations.

The alteration box plot is a useful way of discriminating geochemical trends due to diagenetic alteration from those due to hydrothermal alteration directly related to massive sulfide ores (Fig. 8). The common diagenetic minerals, albite, K feldspar, calcite, and epidote plot on the left hand CCPI axis or the lower AI axis. This contrasts with the common proximal hydrothermal minerals, sericite, chlorite, pyrite, dolomite, and ankerite, which plot on the right hand CCPI axis and the upper AI axis. Thus a diagonal line joining epidote to K feldspar

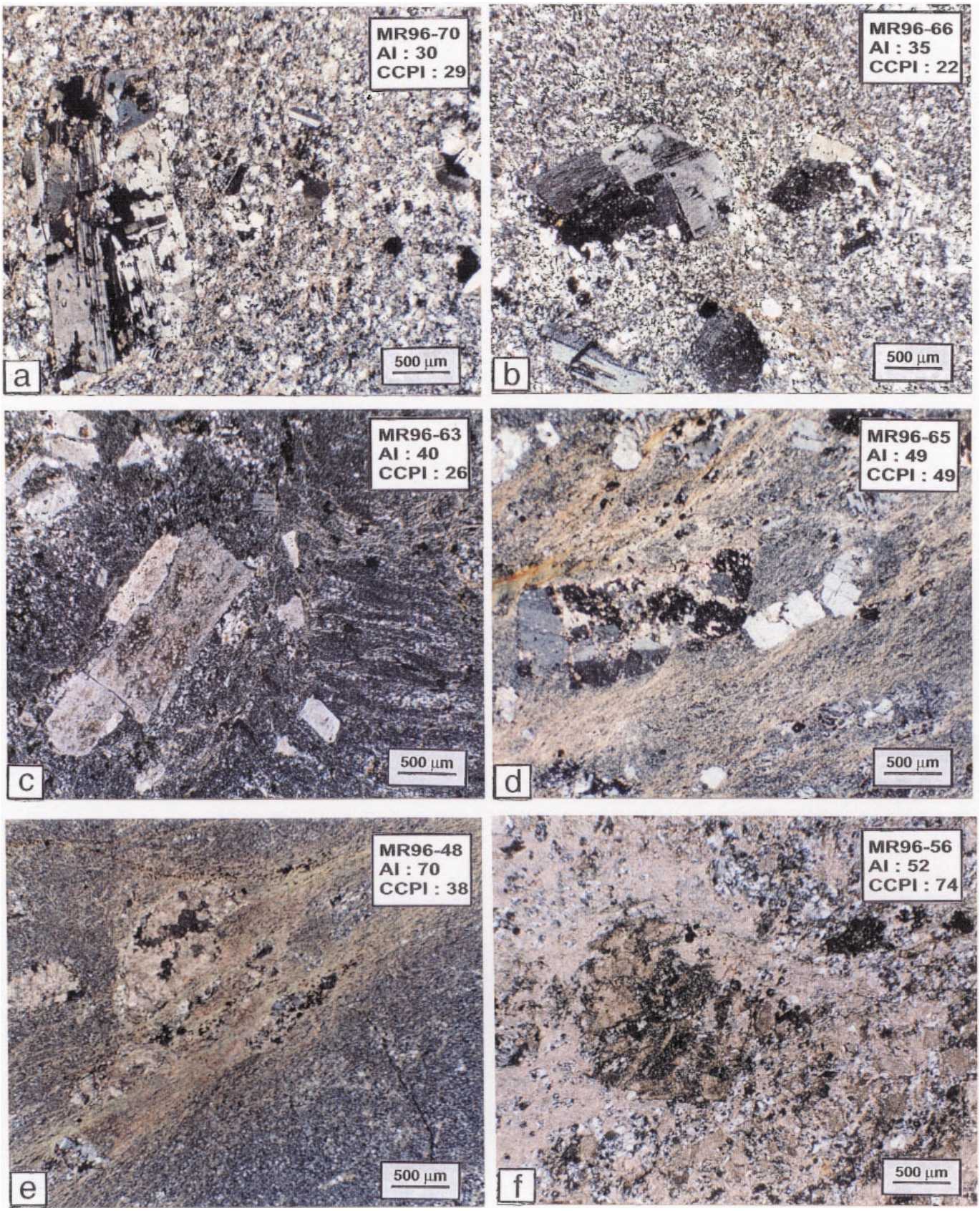

FIG. 6. Photomicrographics of rhyolitic volcanic rocks from the Hercules area, displaying increasing intensity of hydrothermal alteration. These same samples are plotted in Figures 4 and 5 for comparison.

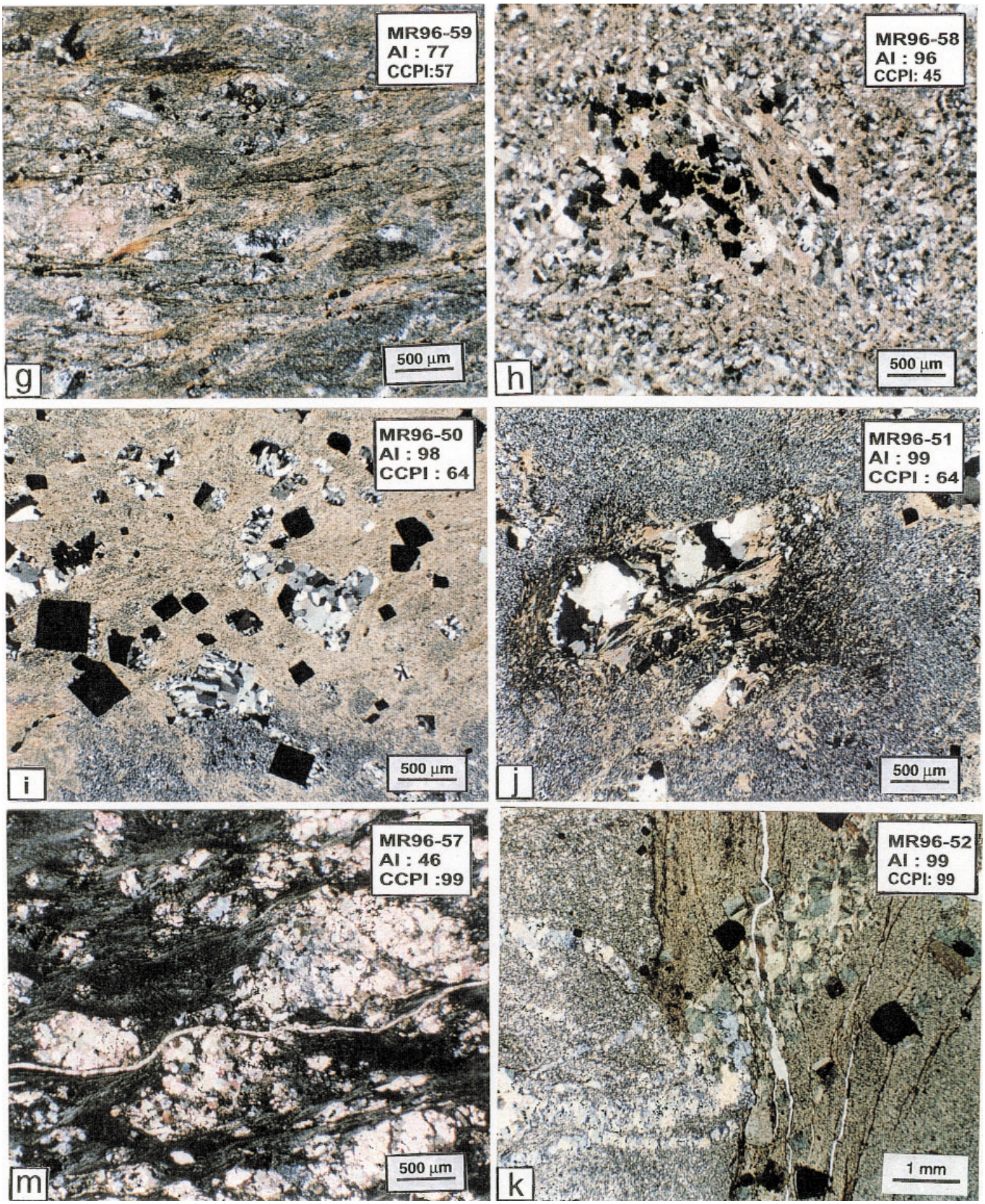

FIG. 6. *(Cont.)*

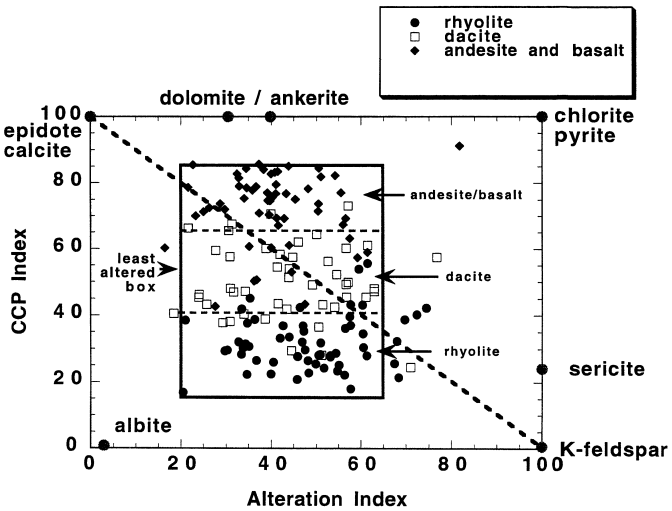

FIG. 7. Fields of least altered volcanics for felsic, intermediate, and mafic compositions. Data from the Rosebery, Que River, and Hellyer areas of the Mount Read Volcanics (Blake et al., unpub. data).

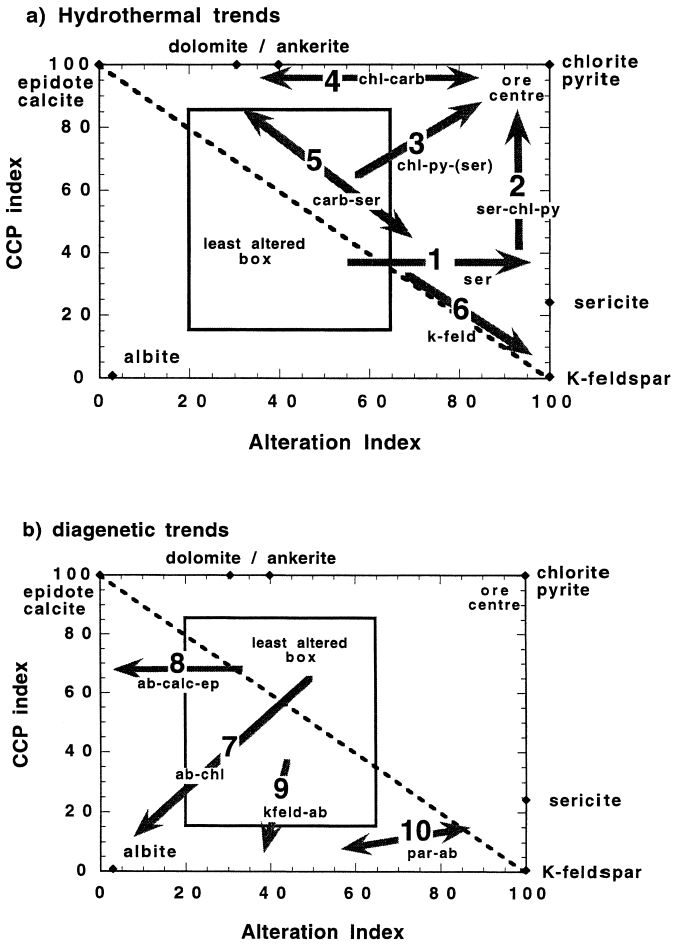

FIG. 8. Fields for diagenetic alteration (lower left) and hydrothermal alteration (upper right) in the alteration box plot. The arrows show the common trends for (a) hydrothermal alteration and (b) diagenetic alteration, described in the text.

effectively separates the field of hydrothermal alteration (upper right) from the field of diagenetic alteration (lower left) in the diagram (Fig. 8). Within these two fields it is possible to identify common trend lines associated with particular styles of hydrothermal and diagenetic alteration.

Hydrothermal trends shown in Figure 8a

Trend 1: Weak sericite alteration at the margins of a hydrothermal system in felsic volcanic host rocks (both hanging wall and marginal footwall to ore)

Trend 2: Intense sericite-chlorite ± pyrite alteration typical of the proximal footwall alteration system to a VHMS deposit, within both felsic and mafic volcanics.

Trend 3: Chlorite ± sericite ± pyrite alteration typical of chlorite-dominated footwall alteration either in felsic or mafic volcanics.

Trend 4: Chlorite-carbonate alteration typically developed immediately adjacent to massive sulfide lenses in a footwall position in either felsic or mafic host rocks (e.g., Hellyer, Hercules).

Trend 5: Sericite-carbonate alteration—immediate hanging wall to massive sulfide or along the favorable stratigraphic host unit, (e.g., Rosebery, Hercules, Hellyer).

Trend 6: K feldspar-sericite—an uncommon trend developed locally within felsic footwall volcanics (e.g., Thalanga; Paulick et al., 2001).

Diagenetic trends shown in Figure 8b

Trend 7: Albite-chlorite, typical of seawater interaction at low temperatures (e.g., spilites and keratophyics; Hughes, 1972; Seyfried and Bischoff, 1979).

Trend 8: Epidote-calcite ± albite—common in intermediate and mafic volcanics (e.g., Gemmell and Fulton, 2001)

Trend 9: K feldspar-albite—early diagenetic trend of K feldspar replacing albite (e.g., Gifkins and Allen, 2001)

Trend 10: Paragonitic sericite-albite—a diagenetic trend recorded in the hanging-wall volcaniclastics at Rosebery (Herrmann et al., 2001).

These trends account for most of the lithogeochemical and mineralogical patterns (or zones) present in submarine volcanic-hydrothermal systems. Transitional zones (e.g., the boundary between marginal hydrothermal and regional diagenetic alteration) or complex overprinting (e.g., diagenesis, hydrothermal alteration, and subsequent metamorphism) should be distinguishable, provided geochemical data for a sufficient range of samples are available to enable trends to emerge in the box plot.

Recent studies (e.g., Callighan, 2001; Gemmell and Fulton, 2001) suggest that albite alteration may be a significant feature of the distal hanging-wall alteration associated with VHMS deposits. Methods to distinguish regional diagenetic albite alteration from VHMS-related distal hydrothermal albite alteration are thus critical for mineral exploration.

Case Studies

A series of case studies, using examples described in more detail elsewhere in this special issue, are considered briefly below to provide further evidence of the usefulness of this approach.

Case study 1: Rosebery VHMS deposit

The Rosebery deposit consists of a series of stratiform Zn-Pb-Cu-Ag-Au-bearing massive sulfide lenses hosted by rhyolitic volcanics, volcaniclastics, and pumice breccias. A comprehensive study of the alteration mineralogy and geochemistry related to the B and K lenses at Rosebery is given by Large et al. (2001). These ore lenses are typically surrounded by an inner Mn carbonate-rich zone, which is developed in the immediate hanging wall and lateral to the ore lenses (Fig. 9). An intense chlorite rich zone occurs in the footwall and is most prominent below the copper-rich ore lenses. The chlorite occurs in a narrow strata-bound sheet rather than the more typical crosscutting pipe zone (Fig. 9). Enveloping the inner carbonate and chlorite zones is a broad lenticular zone of sericite-rich alteration that penetrates deeply into the footwall (up to 100 m) and less than 20 m into the hanging-wall volcanic rocks. The sericite alteration extends along the favorable ore stratigraphy over 500 m along strike from the ore lenses. The sericite zone has an inner core of intense quartz-sericite-pyrite alteration and an outer halo of less intense sericite-Mn carbonate ± chlorite.

Microprobe analyses of the major alteration minerals at Rosebery (sericite, chlorite, and carbonate; Blake et al., unpub. data) have been plotted on the alteration box plot in Figure 10a. Sericite shows significant compositional variation, with two types evident (Herrmann et al., 2001): phengites that plot along the sericite-chlorite join and paragonitic sericite (of diagenetic origin?) that plots on a line between sericite and albite. The chlorites have an Mg/Mg + Fe range of about 0.2 to 0.7 (Large et al., 2001) and plot in a tight cluster at the right-hand top corner of the diagram. The carbonates are of two types (Large et al., 2001): Mn-rich carbonate (rhodocrosite, manganosiderite, kutnahorite, ankerite) of a hydrothermal origin, which plots along the top AI axis; and calcite (low Fe, Mg, Mn) principally confined to synmetamorphic veins, which plots near the left-hand top corner of the box plot (Fig.10a).

Lithogeochemical data from a series of drill holes through the B and K lens host rocks (Large et al., 2001) is plotted in Figure 10b. This data can be grouped into five major fields in the diagram, which relate to the alteration zones described above and in Figure 9.

Field 1: Least altered rhyolitic volcanics fall within a box bounded by an AI = 20 to 65 and a CCPI = 20 to 45.

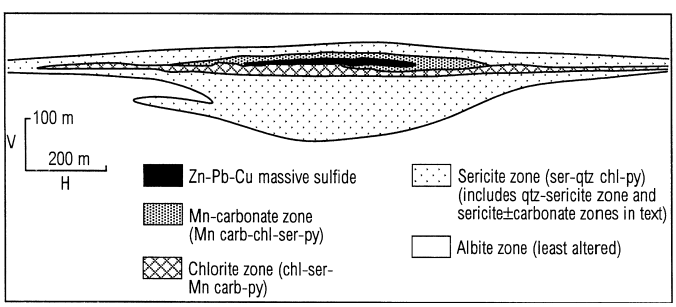

FIG. 9. Diagrammatic model of alteration mineral zones surrounding the Rosebery K lens. Note the relationship between the five alteration zones and the fields defined in the alteration box plot in Figure 10b.

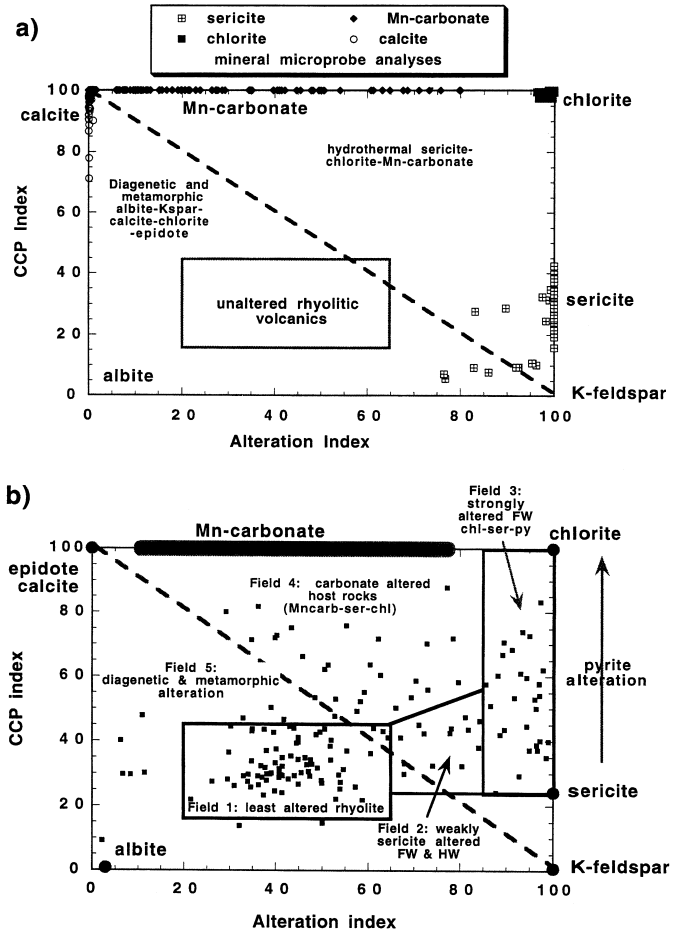

FIG. 10. Alteration box plots for Rosebery VHMS alteration zones (data from Large et al., 2001). a. Microprobe analyses of alteration minerals (sericite, chlorite, carbonate) from DDH 120R and 109R. b. Whole-rock data showing the classification into least altered and the various hydrothermal alteration fields relevant to the Rosebery deposit.

Field 2: Weak sericite alteration in the deep footwall or near hanging wall to the ore lenses has 65 < AI < 85 and 25 < CCPI < 50. This corresponds with trend 1 in Figure 8.

Field 3: Intense footwall alteration typically exhibits AI > 85 and 25 < CCPI < 85, corresponding to trend 2 in Figure 8.

Field 4: Altered rocks within the Rosebery ore horizon, along strike from ore, fall in the truncated triangular field (carbonate-sericite ± chlorite), where the AI varies from 30 to 85 and the CCPI from 50 to 90. Rocks in this field include trends 3 and 5 in Figure 8.

Field 5: Diagenetically altered volcanics, where albite ± calcite ± K feldspar assemblages are well removed from mineralization, show an AI <50, and occur below the epidote-K feldspar join.

In order to test the usefulness of the fields defined in Figure 10b in the exploration context, we studied drill hole DDH 109R that lies 500 m north and along strike from the B lens (Large et al., 2001, Figs. 2 and 3). This drill hole intersects the hanging-wall rhyolitic volcaniclastic mass flows and black slates and the footwall rhyolitic pumice breccias (Fig. 11). The ore position is marked by a weakly altered volcanic sandstone unit. The downhole AI (Fig. 11) shows elevated values

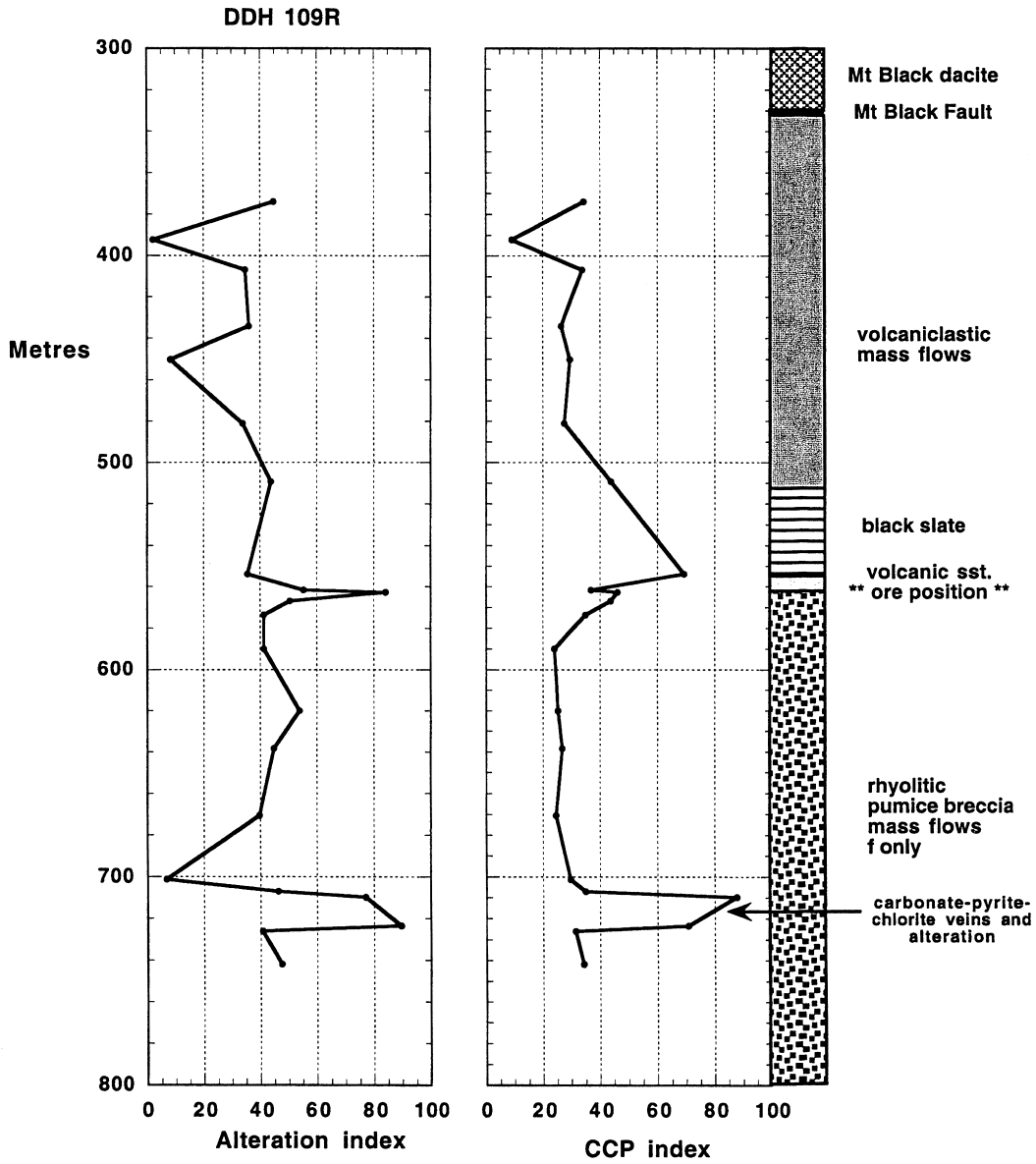

FIG. 11. Downhole variation in the AI and the CCPI for DDH 109R, which intersects the favorable ore-bearing stratigraphy at Rosebery 500 m along strike from the B lens mineralization (Large et al., 2001, fig. 2).

(>60) corresponding to the altered volcanic sandstone and a zone of carbonate-pyrite-chlorite veining and alteration 150 m below the ore position in the rhyolitic pumice breccias. The alteration box plot for this drill hole (Fig.12) shows that most of the samples plot within the box defined for least altered rhyolites (AI = 20–65, CCPI = 15–45). Samples that plot in the upper-right hydrothermal field include the weakly altered volcanic sandstone (ore position), the carbonate-pyrite-chlorite zone in the footwall, and a sample of black slate overlying the volcanic sandstone. All four samples would be assigned high priority for exploration follow-up based on this assessment. Within the diagenetic alteration field (lower left, Fig. 12) one strongly albitized sample and two calcite-albite altered samples plot outside the least altered box. This exercise, carried out on samples from DDH 109R, indicates the value of the alteration box plot in identifying anomalous samples for attention and relating them to the hydrothermal zonation in a well-studied alteration system such as Rosebery.

Case study 2: Thalanga Zn-Pb-Cu-Ag deposit

Thalanga is a metamorphosed stratiform sea-floor VHMS deposit in the Mount Windsor Volcanics of north Queensland. The ore lenses occur at the contact between footwall rhyolites and hanging-wall dacites and andesites. Detailed studies of hydrothermal alteration associated with the deposit are provided by Paulick et al. (2001) and Herrmann and Hill (2001). In brief, the footwall rhyolites are cut at a low angle to the favorable horizon by tabular zones of chlorite-pyrite and pyrite-quartz-sericite that merge toward the top of the rhyolite package, forming an irregular and intensely altered stratabound zone developed immediately below the ore lenses (Fig. 13). The intense chlorite-and sericite-rich feeder zones

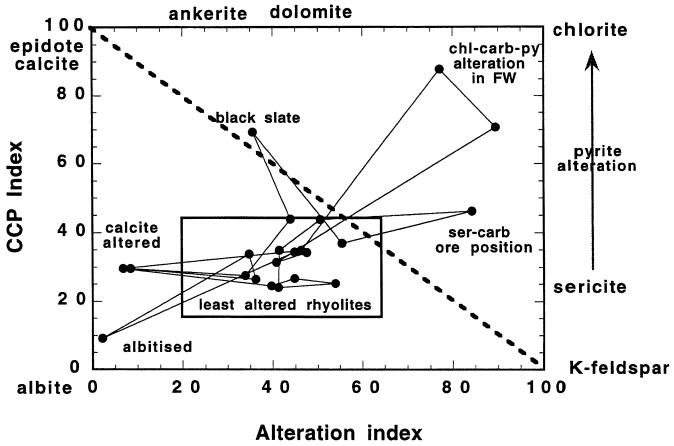

FIG. 12. Alteration box plot for Rosebery DDH 109R samples (Fig. 11). Adjacent samples are joined by lines. Anomalous samples that plot outside the least altered box have been identified and can be related to the lithological log in Figure 11.

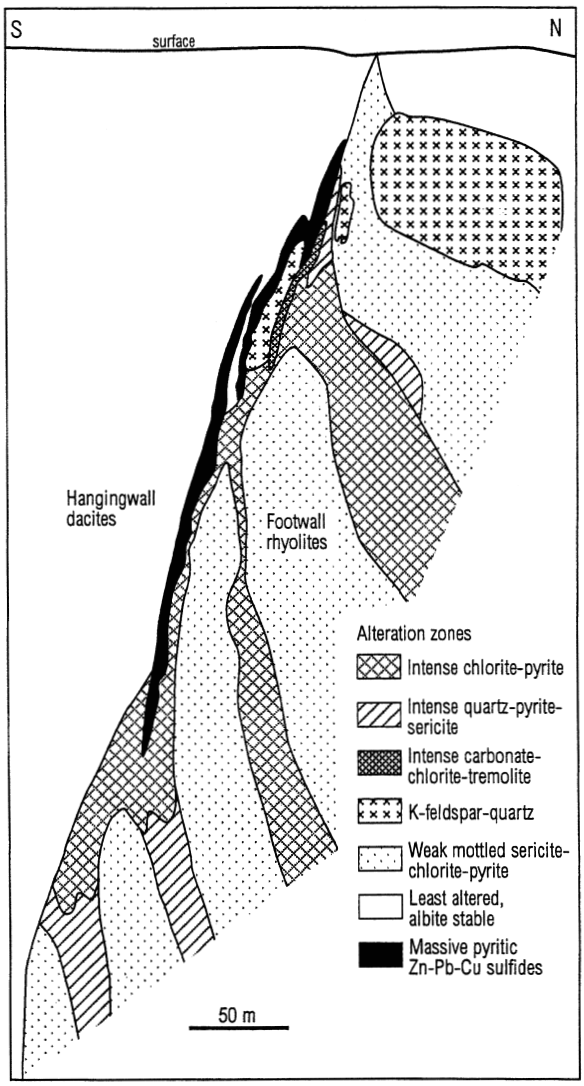

FIG. 13. Simplified alteration zones surrounding the Thalanga deposit (based on the East Thalanga orebody. From Paulick et al. (2001).

are surrounded by a broad low-intensity alteration halo of mottled sericite-chlorite ± pyrite. Small bodies of intensely altered white rhyolite composed of quartz-K feldspar alteration exist below or adjacent to some of the ore lenses. Massive to semimassive zones of carbonate-chlorite-tremolite alteration commonly exist lateral to the ore lenses at the same stratigraphic level (Herrmann and Hill, 2001). Very low intensity alteration in the hanging-wall dacites consists of pervasive patchy albite alteration and fracture-controlled epidote-actinolite-hematite alteration (Paulick et al., 2001).

Lithogeochemical data from a series of drill holes through the Thalanga alteration system (Paulick et al., 2001; Herrmann and Hill, 2001) are plotted in Figure 14. The least altered volcanics, which vary from rhyolitic compositions in the footwall to dacitic and andesitic compositions in the hanging wall, plot within a central field of the box plot (Fig. 14). Four principal hydrothermal alteration trends are evident from this diagram and relate to the trends previously outlined in Figure 8: (1) sericite ± chlorite alteration in the footwall zone distal from ore (trend 1), (2) chlorite-sericite-pyrite alteration of high intensity which corresponds to the footwall feeder zones (trend 2), (3) carbonate-chlorite alteration representing the strata-bound calc-silicate zones lateral to ore (trend 3), and (4) K feldspar alteration in the footwall white rhyolite zones (trend 4). The field of albite alteration in the hanging-wall dacites (Fig. 13) is typical of diagenetic albite trends observed elsewhere (Fig. 8, trend 7).

This case study highlights the value of the alteration box plot in being able to determine a series of lithogeochemical alteration trends that can be related to the mineralogy and mapped alteration zonation. In fact, the scatter of points in Figure 14 along trend 4 toward the K feldspar corner of the diagram was the first indication that a K feldspar hydrothermal alteration zone was preseant at Thalanga. This zone was later confirmed by petrography and XRD (Paulick et al., 2001).

Case study 3: Hellyer VHMS deposit

Hellyer is a mound-shaped Zn-Pb-rich sea-floor massive sulfide deposit in the Mount Read Volcanics of Tasmania. The

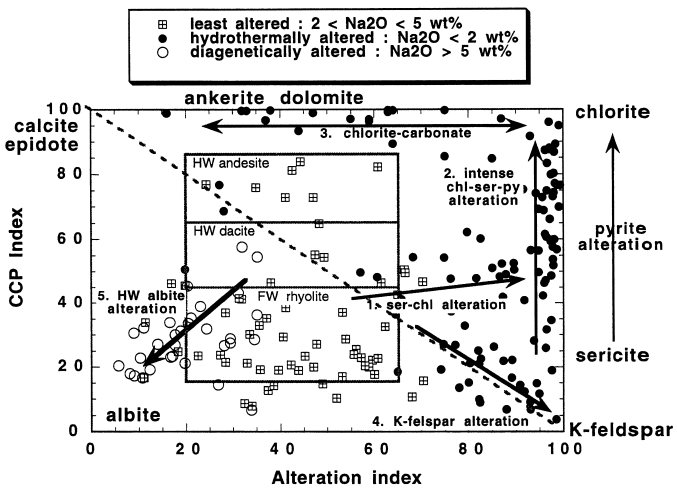

FIG. 14. Alteration box plot for volcanics hosting the Thalanga VHMS deposit, North Queensland. Lithogeochemical data have been provided by Paulick et al. (2001) and Herrman and Hill (2001).

deposit is located at the contact between feldspar-porphyritic andesites in the footwall and pillow basalts in the hanging wall and is a good test case for application of the alteration box plot to understand hydrothermal alteration in mafic volcanic host rocks. Gemmell and Large (1992) have documented a zoned alteration pipe within the andesitic volcanics below the massive sulfide. The pipe contains a core of quartz-rich alteration, surrounded by a chlorite-rich envelope, followed by a sericite-rich envelope, and finally a marginal zone of weak sericite ± chlorite alteration, which merges with the andesite country rock (Fig. 1). A plume of weakly developed calcite-fuchsite ± chlorite alteration extends into the pillow basalts overlying the massive sulfide body and is in turn surrounded by an envelope of quartz-albite alteration (Gemmell and Fulton, 2001).

Lithogeochemical data from a series of drill holes through the footwall andesites and associated alteration pipe are shown in Figure 15. The least altered footwall andesites and basaltic andesites ($2 < Na_2O < 5$ wt %) plot within a field defined by the AI = 20 to 65 and the CCPI = 40 to 85. From the margin toward the center of the alteration pipe, samples show an increase in both the AI and the CCPI, forming a trend toward the chlorite corner of the box plot (Fig. 15). This trend is distinct from that shown by the footwall alteration at both Rosebery (Fig. 10b) and Thalanga (Fig. 14). In the latter two cases the dominant footwall alteration trend is aligned vertically, parallel to the CCPI axis, corresponding to the ser-chl-py trend 2 in Figure 8a. At Hellyer the dominant trend is diagonal from the least altered andesite field to the chlorite corner (chl-py ± ser trend 3 in Fig. 8a). This difference highlights the fact that the Hellyer footwall alteration is dominated by chlorite-bearing assemblages in mafic volcanics, whereas the Rosebery and Thalanga footwall alteration zones are both dominated by sericite-rich assemblages in felsic volcanic host rocks. However in all cases, the most chlorite-rich footwall alteration commonly occurs proximal to the ore lenses (shown as the "ore center" in Fig. 8a).

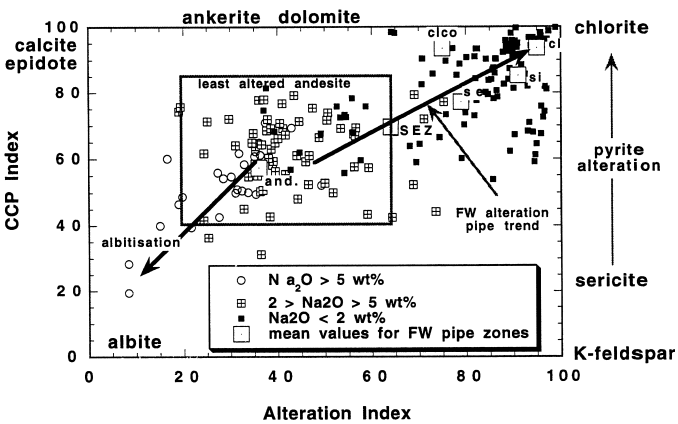

FIG. 15. Alteration box plot for the footwall alteration zone to the Hellyer VHMS deposit (data from Gemmell and Large, 1992; Gemmell, unpub. data). Mean values for footwall pipe alteration zones are also plotted Abbreviations: and = least altered andesite, cl = chlorite ± pyrite ± quartz, clco = chlorite > dolomite, se = strong sericite-chlorite ± pyrite, SEZ = weak sericite ± chlorite, si = quartz–chlorite ± sericite (see Fig. 1)

Case study 4: Western Tharsis Cu-Au deposit

The Western Tharsis deposit is one of a group of disseminated and stockwork Cu-Au deposits in the Mount Lyell district of western Tasmania. Recent research by Huston and Kamprad (2001) on the zonation of alteration assemblages at this deposit suggests that Western Tharsis has more affinities to high-sulfidation epithermal Cu-Au systems than classic VHMS systems. The disseminated chalcopyrite-pyrite ores are hosted by intensely altered quartz-chlorite-sericite schists after felsic to intermediate volcaniclastic rocks and lavas. The ore zone is surrounded by a quartz-sericite altered envelope that passes into a halo of carbonate-chlorite-sericite altered rocks. A zone containing abundant advanced argillic alteration assemblages, including pyrophyllite, topaz, zunyite, and woodhouseite, wraps around the orebody in the inner part of the quartz-sericite envelope (Fig. 16).

Figure 17 contains box plots showing the variations in the AI and the CCPI for both felsic and intermediate volcanic and volcaniclastic rocks at Western Tharsis. Analyses of sedimentary rocks were not plotted as sedimentary processes can

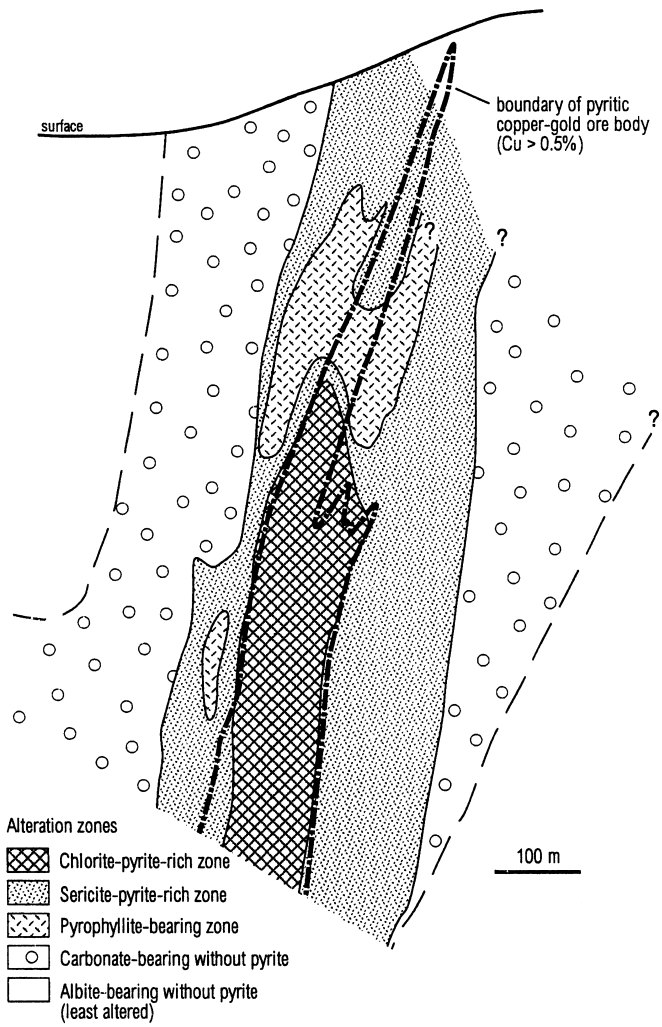

FIG. 16. Simplified sketch of the major alteration zones at the Western Tharsis deposit, western Tasmania. Modified from Huston and Kamprad (2001).

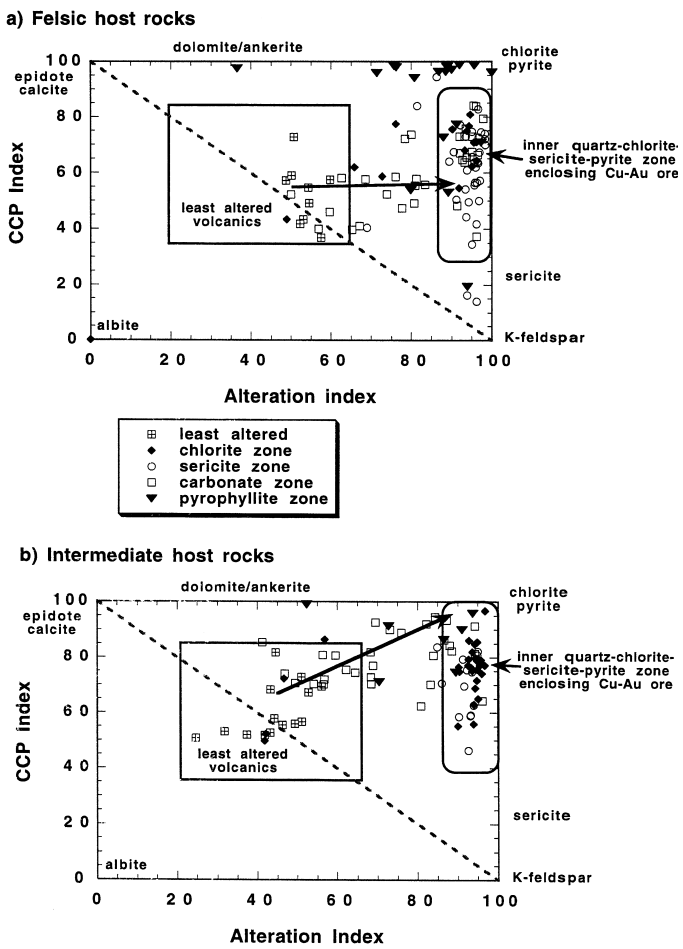

FIG. 17. Alteration box plots for lithogeochemical data from the Western Tharsis Cu-Au deposit. a. Felsic volcanic host rocks. b. Intermediate volcanic host rocks.

significantly affect the AI and CCPI of unaltered rocks, as discussed later. Felsic rocks were distinguished from intermediate rocks using a Zr/TiO_2 ratio of 0.05, however it is recognized that this approach is unlikely to be effective in the advanced argillic (pyrophyllite) alteration zone where TiO_2 and/or Zr may be locally mobile.

The analyses plotted in Figure 17 were classified, depending on mineralogy observed in drill core and/or determined by PIMA analyses, into four alteration types: (1) carbonate (largely ankerite and siderite)-bearing samples that occur exclusively in the outer carbonate-bearing halo, (2) chlorite-bearing samples that lack carbonate and occur mainly in the chlorite-altered ore zone, (3) samples containing advanced argillic mineral assemblages (pyrophyllite, topaz, and zunyite), and (4) sericite-bearing samples that lack chlorite and carbonate. Alteration type (1) was further split into two groups based on Na_2O content, with samples containing more than 1.5 percent Na_2O separated out as the least altered group.

Na_2O-rich, least altered samples plot in a field with an AI between 20 and 65, and a CCPI between 35 and 85. Least altered intermediate rocks tend to have a lower AI but a higher CCPI, which is consistent with observations made on least altered volcanic rocks elsewhere in the Mount Read Volcanics (Fig. 3). Carbonate-altered rocks trend from this least altered field toward the right-hand side of the box plot in both cases, although the trend is toward lower CCPI values in felsic rocks (~55) relative to intermediate rocks (~100). These trends probably correspond to trends (1) and (3) in Figure 8 and relate to the fact that sericite-carbonate assemblages are common in the altered felsic volcanic host rocks, compared to chlorite-carbonate assemblages in the intermediate volcanic host rocks.

The more intensely altered samples tend to plot toward the right and upper margins of the box plot, corresponding to trend (2) in Figure 8. In this region chlorite- and sericite-bearing samples that lack carbonate overlap, although the sericitic samples tend to have a wider range in the CCPI. With the exception of a few samples that may form part of the outer carbonate halo, most chlorite-bearing samples plot within a restricted field with an AI >85 and a CCPI >50; as with least altered samples, the intermediate chlorite-rich samples tend to have higher CCPI values than the felsic samples (e.g., max values of 97 and 81, respectively).

Sericitically altered samples mostly have AI values in excess of 85 but have a wide range in CCPI values (10–95), particularly in felsic samples. This large range in felsic samples must reflect the abundance of pyrite in the samples, as petrographic studies indicate chlorite and carbonate minerals are minor or lacking in this alteration facies, whereas pyrite exhibits a variable distribution commonly above 5 wt percent.

Of the deposits presented here as case studies, advanced argillic assemblages are developed only at the Western Tharsis deposit. Most samples that contain pyrophyllite and other advanced argillic minerals are characterized by high CCPI values (>75; commonly >95 in felsic samples) but variable AI values (35–100). The variability in the AI is caused by the extreme depletion of Na_2O, K_2O, CaO, and MgO noted in many advanced argillically altered samples (Huston, in review): the losses in CaO and Na_2O, which shift the AI to higher values proximal to VHMS deposits, are masked by concomitant losses of MgO and K_2O. Hence, sole dependence on the AI in these advanced argillically altered rocks could be misleading, as highly altered rocks in two instances would be classified as least altered (Fig.17).

The general high CCPI in the pyrophyllite-bearing samples is caused by the lack of K_2O and Na_2O combined with the presence of pyrite in most samples. Samples that have a lower CCPI probably also contain sericite as a significant alteration mineral and may be considered as intermediate between the sericite-bearing assemblage and the advanced argillic assemblage.

The Western Tharsis deposit illustrates many of the advantages and limitations of the alteration box plot. In particular, this plot effectively defines least altered samples and alteration trends at Western Tharsis, although account must be taken of the original composition of the rock. However, although in most cases the trends at Western Tharsis are similar to VHMS deposits in Tasmania and Queensland, significant differences exist in interpreting advanced argillic assemblages within the context of the box plot. Using the trends presented in Figure 8, the pyrophyllite-bearing assemblages would be misclassified as resulting from chlorite-carbonate alteration; however they would be interpreted correctly as an alteration

facies commonly developed close to ore. Hence, use of the box plot for advanced argillic assemblages requires a clear understanding of alteration mineralogy and examination of the absolute abundance of the oxides that constitute the two alteration indexes.

Comparison to Previous Lithogeochemical Methods

Previous geochemical methods developed to study hydrothermal alteration have focused on the chemical gains and losses associated with alteration of the original rocks. Gresens (1967) developed a method to calculate chemical gains and losses by assuming that one or more components of the rock are immobile during the alteration process (Leitch and Lentz, 1994). This was further modified by Grant (1986) who proposed the isocon plot to allow a direct visual graphical comparison of gains and losses for major and trace elements, assuming either constant volume or constant immobile elements (e.g., Al_2O_3, Ti, and Zr). For the study of alteration in complex volcanic sequences, Maclean and Kranidiotis (1987) and Barrett and Maclean (1994) demonstrated the use of incompatible high field strength elements (e.g., Y, Th, Zr, and Yb) to distinguish primary volcanic rock affinities and quantified the related alteration changes from immobile-mobile element relationships. This approach enables chemostratigraphic correlations to be made in highly altered volcanic succession and the determination of elemental mass changes that provide hydrothermal vectors to mineralization (Barrett and Maclean, 1994).

Another lithogeochemical approach developed by Russell and Stanley (1990) and Stanley and Madeisky (1994) uses molar ratios of mobile and/or incompatible immobile elements (Pearce element ratios (PER), e.g., Al/Zr) to distinguish igneous fractionation trends and volcanic component mixing trends from hydrothermal alteration trends. The PER technique does not require a knowledge of the unaltered precursor volcanic rock and is a rigorous mathematical approach to the quantification of alteration and igneous fractionation in a suite of volcanic rocks (Stanley and Madeisky, 1994).

These previous lithogeochemical methods were designed initially to provide information on the precursor igneous rock composition and to quantify the chemical gains and losses associated with the alteration. Although this information is important in the exploration context it does not readily provide a vector to mineralization. The alteration box plot on the other hand has been designed specifically to assist exploration targeting of VHMS ores. The advantages of the box plot compared to these previous techniques are the following:

1. Only major element whole-rock analyses are required, compared to other techniques that use both major and immobile trace elements.
2. The mathematical computations are very simple, requiring only the determination of the two alteration indexes, which are then plotted on an X-Y graph. There is no need to determine igneous fractionation trends or compute element gains and losses.
3. Interpretation of the data is straightforward; altered samples plot in arrays extending from the least altered box toward the dominant alteration mineral positions. The intensity of alteration is indicated by the relative displacement of samples from the least altered box.
4. Proximal hydrothermal alteration trends can be readily distinguished from distal alteration trends and from regional diagenetic alteration.

The main strength of the alteration box plot is that it is a simple and rapid technique, which relates whole-rock lithogeochemistry to alteration mineralogy, at the same time providing information on the intensity of alteration and relationship of given sample sets to the classic zonation patterns observed around VHMS deposits. It is not a substitute for more rigorous mathematical treatments that determine igneous fraction trends and provide quantitative information on chemical gains and losses (e.g., Barrett and Maclean, 1994; Stanley and Madeisky, 1994)

Limitations of the Alteration Box Plot

There are a number of limitations of this method of which potential users need to be aware:

1. Because neither the AI nor the CCPI include SiO_2, the box plot cannot provide any measure of quartz content in the alteration assemblage. Silica alteration is important in some VHMS systems, such as the core zone of the Hellyer alteration pipe (Gemmell and Large 1992), in the stockwork zone of some Kuroko deposits (e.g., Shirozo, 1974), and in some Cyprus-type alteration pipes (e.g., Lydon, 1984). Intensely silicified footwall altered volcanics are most likely to plot close to the sericite-chlorite join on the right-hand side of the box plot (trend 2 in Fig. 8) as shown in the footwall silica core zone at Hellyer (Fig. 15) and the Western Tharsis inner quartz-rich alteration zones (Fig. 17).
2. The box plot is only recommended for the study of alteration in primary volcanic rocks—lavas, subvolcanic intrusion, or volcaniclastics. Volcanic-derived sediments should be plotted with extreme caution. Erosion and transport processes involved in sedimentation lead to chemical changes (commonly loss of alkalies), causing increases in both the AI and the CCPI that are unrelated to hydrothermal alteration. Sedimentary processes thus cause a spread of primary compositions across the box plot that render it meaningless for alteration studies. This problem is not unique to the box plot but is common among almost all lithogeochemical alteration methods. The effect is apparent in Figure 12, where the unaltered hanging-wall black slate at Rosebery is seen to plot in the hydrothermal alteration field above the epidote-K feldspar join.
3. The box plot is most suited to the study of hydrothermal alteration in felsic volcanics rather than mafic volcanics. In the former, there is a good separation of the unaltered felsic volcanic field from the hydrothermal fields represented by the upper-right part of the plot, and consequently alteration trends can be clearly defined (e.g., Figs. 7, 8a, and 10). This contrasts with mafic volcanics, where the unaltered field has greater CCPI values and shows considerable overlap with the hydrothermally altered field, making the distinction between altered and unaltered volcanics more difficult (e.g., Figs. 7, 8a, and 15). This problem becomes more obvious in the study of weak intensity hanging-wall alteration. For example, in the felsic volcanic-hosted Rosebery system the hanging-wall sericite alteration can be readily identified (Fig. 10b, field 2);

however, in the mafic volcanic-hosted Hellyer system the hanging-wall fuchsite-carbonate alteration field overlaps with the least altered andesite-basalt field and cannot be easily resolved (Gemmell and Fulton, 2001, fig. 13).

4. The box plot was developed for the study of alteration associated with VHMS systems. It is not appropriate for the study of alteration related to other ore types, such as porphyry Cu, epithermal Au, or sediment-hosted deposits. As with most other lithogeochemical techniques it is not useful in the study of advanced argillic alteration trends.

5. The alteration box plot should not be used in isolation but is most powerful in the understanding of alteration when combined with petrographic and/or mineralogical studies (XRD or PIMA). Used in this way, the box plot reveals trends in the data, from least altered to strongly altered, that can be related to exploration targets.

Conclusions

Hydrothermal alteration related to VHMS ore systems principally involves the breakdown of plagioclase and volcanic glass in the primary volcanic host rocks and their replacement by sericite, chlorite, carbonate, pyrite, and quartz in varying propositions, depending on the zonal pattern of the individual hydrothermal system under study. The vast literature available on hydrothermal zonation associated with sea-floor massive sulfide deposits indicates that there are consistent patterns of zonation, with chlorite-, pyrite-, and sometimes carbonate- and quartz-rich assemblages close to ore, surrounded by halos of sericite-rich and sericite ± chlorite ± carbonate assemblages. The alteration box plot has been devised as a simple lithogeochemical technique to assess the intensity of VHMS-related hydrothermal alteration and to place samples within the context of the normal mineralogical zonation exhibited by the hydrothermal systems. By plotting the alteration index (AI) against the chlorite-pyrite-carbonate index (CCPI) for a range of volcanic rock samples from a given locality, prospect, or deposit it is possible to readily separate them into three groups: (1) least altered, (2) diagenetically altered, and (3) hydrothermally altered. The plot enables the relationship between alteration mineralogy and lithogeochemistry to be explored and to place the samples within the context of a zoned hydrothermal alteration system. Ten different mineralogical trends have been defined in the diagram, six of which relate to common hydrothermal alteration trends and four of which relate to diagenetic alteration trends. Used in conjunction with petrographic and mineralogical studies the alteration box plot becomes a powerful tool to assist in the understanding and exploration of VHMS-related hydrothermal systems.

Acknowledgments

This research was funded by the Australian Mineral Industry Research Association (AMIRA) and the Australian Research Council (ARC). Thanks to the mining company personnel that participated in the project and to the members of the CODES research team that stimulated discussion on the topic of hydrothermal alteration. Two *Economic Geology* reviewers, John Thompson and Scott Halley, are thanked for their very useful comments on how to improve the manuscript.

REFERENCES

Allen, R.L., and Cas, R.A.F., 1990, The Rosebery controversy: Distinguishing prospective submarine ignimbrites-like units from the subaerial ignimbrites in the Roseberry-Hercules Zn-Cu-Pb massive sulphide district, Tasmania [abs.]: Australian Geological Convention, 10th, Hobart, Geological Society of Australia, Abstracts 25, p. 31–32.

Ashley, P.M., Dudley, R.L., Lesh, R.H., Marr, J.M., and Ryall, A.W., 1988, The Scuddles Cu-Zn prospect, an Archean volcanogenic massive sulfide deposit, Golden Grove district, Western Australia: Economic Geology, v. 83, p. 918–951.

Barrett, T.J., and Maclean, W.H., 1994, Chemostratigraphy and hydrothermal alteration in exploration for VHMS deposits in greenstones and younger volcanic rocks: Geological Association of Canada Short Course Notes, v. 11, p. 433–467.

Corbett, K.D., 1986, Geology of the Henty River-Mt. Read area: Tasmania Department of Mines, Mt. Read Volcanics project, Map 3.

Date, J., Watanabe,Y., Iwaya, S., and Horiuchi, M., 1979, A consideration of the alteration of the dacite below the Fukazawa ore deposit, Fukazawa mine, Akita Prefecture: Mining Geology, v. 29, p. 187–196 (in Japanese with English abs.).

Date, J., Watanabe, Y., and Saeki, Y., 1983, Zonal alteration around the Fukazawa Kuroko deposits, Akita Prefecture, northern Japan: Economic Geology Monograph 5, p. 365–386.

Eastoe, C.J., Solomon, M., and Walshe, J.L., 1987, District-scale alteration associated with massive sulfide deposits in the Mount Read Volcanics, western Tasmania: Economic Geology, v. 82, p. 1239–1258.

Franklin, J.M., Kasarda, J., and Poulson, K.H., 1975, Petrology and chemistry of the alteration zone of the Mattabi massive sulfide deposit: Economic Geology, v. 70, p. 63–79.

Franklin, J.M., Lydon, J.W., and Sangster, D.F., 1981, Volcanic-associated massive sulfide deposits: Economic Geology 75th Anniversary Volume, p. 485–627.

Gemmell, J.B., and Fulton, R., 2001, Geology, genesis, and exploration implications of the footwall and hanging-wall alteration associated with the Hellyer volcanic-hosted massive sulfide deposit, Tasmania, Australia: Economic Geology, v. 96, p. 1003–1035.

Gemmell, J.B., and Large, R.R., 1992, Stringer system and alteration zones underlying the Hellyer volcanogenic massive sulfide deposit, Tasmania: Economic Geology, v. 87, p. 620–649.

Gifkins, C.C., and Allen, R.L., 2001, Textural and chemical characteristics of diagenetic and hydrothermal alteration in glassy volcanic rocks: Examples from the Mount Read Volcanics, Tasmania: Economic Geology, v. 96, p. 973–1002.

Grant, J.A., 1986, The isocon diagram—a simple solution to Gresens equation for metasomatic alteration: Economic Geology, v. 81, p. 1976–1982.

Gresens, R.L., Composition-volume relationships of metasomatism: Chemical Geology, v. 2, p. 47–55.

Hashiguchi, H., Yamada, R., and Inoue, T., 1983, Practical application of low Na_2O anomalies in footwall acid lavas for deliminating promising areas around the Kosaka and Fukazawa Kuroko deposits, Akita Prefecture, Japan: Economic Geology Monograph 5, p. 387–394.

Herrmann, W., and Hill, A.P., 2001, The origin of chlorite-tremolite-carbonate rocks associated with the Thalanga volcanic-hosted massive sulfide deposit, North Queensland, Australia: Economic Geology, v. 96, p. 1149–1173.

Herrmann, W., Blake, M., Doyle, M., Huston, D., Kamprod, J., Merry, N., and Pontual, S., 2001, Short wavelength infrared (SWIR) spectral analysis of hydrothermal alteration zones associated with base metal sulfide deposits at Rosebery and Western Tharsis, Tasmania, and Highway-Reward, Queensland: Economic Geology, v. 96, p. 939–955.

Hughes, C.J., 1972, Spilites, keratophyes and the igneous spectrum: Geological Magazine, v. 109, p. 513–527.

Huston, D.L., and Kamprad, J., 2001, Zonation of alteration facies at Western Tharsis: Implications for the genesis of Cu-Au deposits in the Mount Lyell field, western Tasmania: Economic Geology, v. 96, p. 1123–1132.

Iijima, A., 1974, Clay and zeolitic alteration zones surrounding Kuroko deposits in the Hokiroku district, northern Akita, as submarine hydrothermal-diagenetic alteration products: Mining Geology Special Issue, no. 6, p. 267–289.

Ishikawa, Y., Sawaguchi, T., Iwaya, S., and Horiuchi, M., 1976, Delineation of prospecting targets for Kuroko deposits based on modes of volcanism of underlying dacite and alteration halos: Mining Geology, v. 26, p. 105–117 (in Japanese with English abs.).

Large, R.R., 1992, Australian volcanic-hosted massive sulfide deposits: Features, styles, and genetic models: Economic Geology, v. 87, p. 471–510.

Large, R.R., Allen, R.L., Blake, M.D., and Herrmann, W., 2001, Hydrothermal alteration and volatile element halos for the Rosebery K lens volcanic-hosted massive sulfide deposit, western Tasmania: Economic Geology, v. 96, p. 1055–1072.

Leitch, C.H.B., and Lentz, D.R., 1994, The gresens approach to mass balance constraints of alteration systems: Methods, pitfalls, examples, *in* Lentz, D.R., ed., Alteration and alteration processes associated with ore-forming systems: Geological Association of Canada Short Course Notes, Waterloo, Ontario, May 13–15, v. 2, p. 161–192.

Lentz, D.R., 1996, Recent advances in lithogeochemical exploration for massive sulphide deposits in volcano-sedimentary environments: Petrogenetic, chemostratigraphic and alteration aspects with examples from the Bathurst camp, New Brunswick: New Brunswick Department of Natural Resources and Energy, Mineral and Energy Division Mineral Resources Report 96–1, p. 73–119.

——1999, Petrology, geochemistry, and oxygen isotope interpretation of felsic volcanic and related rocks hosting the Brunswick 6 and 12 massive sulfide deposits (Brunswick belt) Bathurst mining camp, New Brunswick, Canada: Economic Geology, v. 94, p. 57–86.

Lydon, J.W., 1984, Some observations on the mineralogical and chemical zonation patterns of volcanogenic sulphide deposits of Cyprus: Geological Survey of Canada Paper 84-1A, p. 611–616.

——1988, Volcanogenic massive sulphide deposits, Part 2: Genetic models: Geoscience Canada Reprints Series 3, p. 155–182.

Maclean, W.H., and Krandiotis, P., 1987, Immobile elements as monitors of mass transfer in hydrothermal alteration: Phelps Dodge massive sulfide deposit, Matagami, Quebec: Economic Geology, v. 82, p. 951–962.

Munha, J., and Kerrich, R., 1980, Sea water basalt interaction in splites from the Iberian pyrite belt: Contributions to Mineralogy and Petrology, v. 73, p. 191–200.

Paulick, H., Herrmann, W., and Gemmell, J.B., 2001, Alteration of felsic volcanics hosting the Thalanga massive sulfide deposit, North Queensland, Australia: Geochemical proximity indicators to ore: Economic Geology, v. 96, p. 1175–1200.

Russell. J.K., and Stanley, C.R., 1990, eds., Theory and application of Pearce element ratios to geochemical data analysis: Geological Association of Canada Short Course Notes, v. 8, 315 p.

Saeki, Y., and Date, J., 1980, Computer application to the alteration data of the footwall dacite lava at the Ezuri Kuroko deposits, Akita Prefecture: Mining Geology, v. 30, p. 241–250 (in Japanese with English abs.).

Sangster, D.F., 1972, Precambrian volcanogenic massive sulphide deposits in Canada: A review: Geological Survey of Canada Paper 72–22, 44 p.

Schardt, C., Cooke, D.R., Gemmell, J.B., and Large, R.R., 2001, Geochemical modeling of the zoned footwall alteration pipe, Hellyer volcanic-hosted massive sulfide deposit, western Tasmania, Australia: Economic Geology, v. 96, p. 1037–1054.

Seyfried, W.E., Jr., and Bischoff, J.L., 1979, Low temperature basalt alteration by seawater an experimental study at 70°C and 170°C: Geochimica et Cosmochimica Acta, v. 43, p. 1937–1947.

Shirozo, H., 1974, Clay minerals in altered wall rocks of the Kuroko-type deposits: Society of Mining Geologists of Japan, Special Issue 6, p. 303–311.

Stanley, C.R., and Madeisky, H.E., 1994, Lithogeochemical exploration for hydrothermal ore deposits using Pearce element ratio analysis: Geological Association of Canada Short Course Notes, v. 11, p. 193–211.